# A theoretical rotationally resolved infrared spectrum for $H_2O^+$ ($X\,^2B_1$)

B. Weis, S. Carter, and P. RosmusH.-J. WernerP. J. Knowles

Citation: The Journal of Chemical Physics **91**, 2818 (1989); doi: 10.1063/1.456951
View online: http://dx.doi.org/10.1063/1.456951
View Table of Contents: http://aip.scitation.org/toc/jcp/91/5
Published by the American Institute of Physics

# A theoretical rotationally resolved infrared spectrum for $H_2O^+$ ($X\,^2B_1$)

B. Weis, S. Carter, and P. Rosmus
*Fachbereich Chemie der Universität, D-6000 Frankfurt, Federal Republic of Germany*

H.-J. Werner
*Fachbereich Chemie der Universität, D-4800 Bielefeld, Federal Republic of Germany*

P. J. Knowles
*School of Chemistry and Molecular Sciences, University of Sussex, Brighton BN1 9QJ, United Kindgom*

(Received 19 December 1988; accepted 25 May 1989)

Three-dimensional potential energy and electric dipole moment functions for the electronic ground state of $H_2O^+$ have been calculated from highly correlated multiconfiguration reference configuration interaction (MRCI) electronic wave functions. The analytic representations of these functions have been used in vibrational and perturbational calculations of the rovibrational absorption spectrum of $H_2O^+$. The quartic force fields in normal coordinates have been employed in the evaluation of the equilibrium spectroscopic constants in $H_2O^+$, $D_2O^+$, and $HDO^+$ by perturbation theory. The equilibrium structure, vibrational band origins, centrifugal distortion constants and rotational energy levels agree very well with the available experimental data. Absolute vibrational band intensities have been calculated from the dipole moment functions and are compared with theoretical integrated band intensities. The radiative lifetimes of excited vibrational states exhibit mode specific variations. The rotationally resolved room temperature absorption spectra have been evaluated *ab initio* for the pure rotational and the $\nu_2$, $2\nu_2$, $\nu_1$, $\nu_3$, and $3\nu_2$ transitions. The rovibrational electric dipole transition matrix elements and absolute line intensities are given for the most intense transitions. These data take full account of anharmonicity effects and vibration–rotation coupling.

## I. INTRODUCTION

In recent years, the $H_2O^+$ cation has been the subject of many experimental studies because of its importance for elementary processes in outer space and the earth's atmosphere. Its electronic ground state $X\,^2B_1$ has been characterized by high resolution emission[1–5] and absorption[6] experiments, by laser magnetic resonance[7] and infrared absorption[8,9] spectroscopy, in low resolution by photoelectron spectroscopy[10–12] and by vibrationally resolved inelastic and charge transfer scattering $H^+$ by $H_2O$.[13,14] The properties of the water cation are of interest in the $H_2 + O^+$ collision dynamics,[15,16] and for the interpretation of the dissociative ionization,[17] Penning ionization,[5] or electron impact processes[18] in water.

To date, high resolution data[2,3,7,9] are available for the vibrational ground state and the $\nu_1$, $\nu_2$, $2\nu_2$, $3\nu_2$, and $\nu_3$ vibrational states for the electronic ground state in $H_2O^+$. New high resolution infrared data for $\nu_2$ have recently become available.[19] For $D_2O^+$ such data exist for the vibrational ground state and the $\nu_2$ and $3\nu_2$ vibrational states.[3] Additional information about higher overtones is available from the photoelectron spectra[10–12] of $H_2O$, $D_2O$, and HDO. Using the $A$–$X$ emission data of Lew,[2] Jungen, Hallin, and Merer[20] derived an effective one-dimensional potential for the bending coordinate. Recently, Dinelli, Crofton, and Oka[9] used relationships between centrifugal distortion and potential constants, as well as the vibrational frequencies, and derived a three dimensional quadratic potential expansion in internal coordinates. In this treatment the anharmonicity of the potential was neglected. There have been several other attempts to determine the $\omega_i$ and $x_{ij}$ constants from the photoelectron spectra[10–12] and from theoretical calculations.[21–24] So far, the most accurate theoretical three dimensional potential energy function for the electronic ground state of $H_2O^+$ is the cubic force field of Esposti.[21] This force field, however, yields stretching frequencies of $H_2O^+$ which deviate from the experimental values by more than 100 $cm^{-1}$. Neither absolute intensity measurements nor the dipole moment function for the electronic ground state of $H_2O^+$ have so far been reported.

In this work we present three-dimensional theoretical near equilibrium potential energy and electric dipole moment functions for the $X\,^2B_1$ state of $H_2O^+$ calculated from highly correlated multiconfiguration reference configuration interaction (MRCI) electronic wave functions. Analytic expansions of these functions have been used to calculate the rovibrational transition energies and absolute vibrational band and line intensities. The vibrational method employed in the determination of the high resolution vibration–rotation spectra takes full account of anharmonicity and vibration–rotation coupling effects.[25,26] The nuclear spin interactions, the electron spin–rotation and the electronic angular momentum–rotation (Renner–Teller effect) couplings have been neglected.

Although the $X\,^2B_1$ and the $A\,^2A_1$ states of the $H_2O^+$ ion form a Renner–Teller pair, we have treated the near equilibrium part of the electronic ground state potential energy function adiabatically as a single state problem. We will report Renner–Teller calculations for $H_2O^+$ in a separate publication.[27] In a series of test calculations including the three-dimensional functions of the expectation values of the $L$

 0021-9606/89/172818-16$02.10 

operators in the rovibronic Hamiltonian[28] we found that the adiabatic approximation for low lying vibrational levels of the electronic ground state is well justified, since the barrier to linearity has been calculated[27] to be rather high, 7948 $cm^{-1}$. The reported[20] empirical value of 9187 $cm^{-1}$ is too high, because its derivation was based on wrong assignments[2,3] of the bending quantum numbers in the $A$ state of $H_2O^+$ and $D_2O^+$. The electron angular momentum–rotation coupling effects hardly influence the stretching frequencies. The bending frequencies for $v_2 = 1$ and 2 of $H_2O^+$ and $D_2O^+$ are affected by only a few wave numbers. Of course, in the regions of the potential close to linear structures such an approach fails and the Renner–Teller coupling effects have to be included. A comparison of the calculated vibrational band origins with all available experimental data shows an excellent agreement with a maximum deviation of 7 $cm^{-1}$ up to about 5000 $cm^{-1}$ above the vibrational ground state (cf. Secs. III and V).

Section II deals with the electronic structure and nuclear motion calculations. In Sec. III the properties related to the near equilibrium potential energy function are discussed. In Sec. IV the electric dipole moment function and its implications for the vibrational radiative probabilities are reported, and, finally, in Sec. V we present purely theoretical rotationally resolved spectra of $H_2O^+$.

## II. ELECTRONIC STRUCTURE AND NUCLEAR MOTION CALCULATIONS

The Gaussian basis set used in the MRCI calculations of the three-dimensional potential energy and electric dipole moment functions comprised 121 primitive basis functions contracted to 80 groups. For the oxygen atom the 13*s*, 8*p* basis of van Duijneveldt[29] was employed with the innermost 7*s* and 4*p* functions contracted together. The basis set was augmented by three *d* functions with exponents 3.6, 1.2, and 0.4 $a_0^{-2}$, and one contracted set of *f* functions with exponent 2.25 and 0.75 $a_0^{-2}$ and contraction coefficients 0.6168 and 0.5278. For hydrogen the 8*s* basis set[29] was used with the 5 functions with the largest exponents contracted together. Three sets of *p* functions with exponents 1.8, 0.6 and 0.2 $a_0^{-2}$ and one set of *d* functions with exponent 0.7 $a_0^{-2}$ were included. We first performed a series of preliminary calculations in which the influence of the size and the composition of the configuration spaces on the shape of the potential energy function and on the barrier to linearity of $H_2O^+$ were tested. The details of this investigation will be published separately.[27]

In order to obtain a molecular orbital basis for MRCI[30,31] calculations, CASSCF[32,33] (complete active space self-consistent field) calculations were performed with an active space of eight molecular orbitals ($2a_1$–$5a_1$, $1b_1$–$2b_1$, $1b_2$–$2b_2$, in $C_{2v}$ symmetry, or their equivalents in $C_s$, $C_{\infty v}$, or $D_{\infty h}$ symmetries). The $5a_1$ and $2b_2$ orbitals correspond to $\pi^*$ orbital in collinear geometries. It was found that the inclusion of these orbitals into the reference space considerably improves the wave functions. In order to obtain a common set of orthogonal molecular orbitals for use in the calculation of transition moments and expectation values of the $L$ operators,[27] the $X\,^2B_1$ and the $A\,^2A_1$ states have been optimized simultaneously in a state average procedure. In the subsequent MRCI calculations the leading configuration and all singly and doubly excited configurations in the active space were used as reference configurations. This selection yielded 89 configurations in $C_s$ symmetry (or their equivalents in higher symmetries) for the electronic ground state of $H_2O^+$. The internally contracted multireference CI calculations were performed using the recently developed new method.[30,31] In $C_s$ symmetry the number of variational parameters in the internally contracted MRCI wave functions was 147 257, which corresponds to more than 1.5 million configurations in equivalent uncontracted MRCI calculations. The dipole moments were calculated as expectation values of the MRCI wave functions.

The nuclear motion problem was solved both by perturbation theory[34] and also by variational[25] calculations. The analytical form of the MRCI potential energy function (cf. Sec. III) was transformed to internal coordinates and by *l*-tensor algebra to dimensionless normal coordinates and the spectroscopic constants, rovibrational energy levels corresponding to the second order perturbation theory were evaluated. Such calculations are extremely fast when compared with variational calculations, but they have the disadvantage that higher order effects are not accounted for. Moreover, the calculation of the rovibrational line intensities becomes very cumbersome if higher than linear terms in the dipole moment expansion are included. This applies especially to the asymmetric rotors.[38] Our variational calculations of the vibration–rotation energy levels and associated wave functions were carried out using the complete nuclear motion Hamiltonian in internal coordinates.[39] In this procedure, the wave function of the vibrational motion is taken as a product of Morse oscillator functions in the symmetric stretch coordinate $R_1 + R_2$, harmonic–oscillator functions in the asymmetric stretch coordinate $R_1 - R_2$ and associated Legendre functions in the valence bond angle. Integration of the Hamiltonian matrix elements is carried out numerically over the vibrational coordinates using Gaussian quadrature. The rotational functions are spherical harmonics in the Euler angles $\beta, \gamma$ since, in the absence of any external field, the $2J + 1$ components of $M$ are strictly degenerate; hence, only those functions with $M = 0$, which are independent of the Euler angle $\alpha$, are chosen. In these functions, $\gamma$ relates the molecules fixed and space fixed $z$ axes, and the molecule fixed frame is such that the $x$ axis always bisects the valence bond angle $\phi$, and $R_1$ lies in the positive $xz$ quadrant. The $y$ axis is, therefore, out of the molecular plane, and is chosen to complete the right-handed coordinate system. Suitable combinations of the rotational functions[28] are taken which transform as irreducible representation of the $C_{2v}$ point group. Each function has its $J$ and $k$ quantum numbers; $k$ repesents the projection of $J$ on the $z$ axis of the internal coordinate system. The integration over the rotational functions is carried out analytically. For the details of the calculations of the dipole moment matrix elements we refer the reader to Ref. 26.

In the following sections, variationally calculated energies and intensities are reported for low vibrational excitations up to $J = 9$. In carrying out these calculations, it was

important to check the degree of convergence of the calculated transition energies and line intensities with respect to the size of the basis set used. First, subsets of the complete Hamiltonian, which only involve matrix elements between the operators diagonal in $k$, were set up. Such matrices were diagonalized for all $k = 0,...,J$ and the resulting "vibrational" wave functions and energies stored. Sets of these functions from each block were then selected for the final diagonalization involving the operators off-diagonal in $k$, such that a total of $N$ functions with the lowest vibrational energies were used in the vibration–rotation matrix. $N$ was systematically increased until the resulting vibration–rotation energy levels had converged. It was found that all rotational levels of the first five vibrational excitations $\nu_2$, $2\nu_2$, $\nu_1$, $\nu_3$, $3\nu_2$ were converged to better than 0.1 $cm^{-1}$ for all $J = 0,...,9$ by this procedure, and this gives us confidence in convergence of the subsequent band intensities to better than about 5%.

## III. NEAR EQUILIBRIUM POTENTIAL ENERGY FUNCTION OF $H_2O^+(X\,^2B_1)$

The calculated MRCI energies for 50 symmetry unique geometries in the vicinity of the equilibrium were fitted to a polynomial expansion in bond stretching and angle bending coordinates:

$$V(Q_1,Q_2,Q_3) = \sum C_{ijk}(Q_1)^i(Q_2)^j(Q_3)^k.$$

For the stretches ($Q_1$ and $Q_2$) Simons–Parr–Finlan coordinates $Q = 1 - r^{ref}/r$ was used, while the bending coordinate $Q_3$ was expressed in terms of a cubic expansion in $\theta = \phi - \phi^{ref}$ as $Q_3 = A_0\theta + A_1\theta^2 + A_2\theta^3$. This coordinate,[40] which is very useful for expansion at bent geometries, was chosen to satisfy the conditions $Q_3(\phi = 180°) = 1$ and $dQ_3(\phi = 180°)/d\phi = 0$. The first condition represents a normalization, the second condition ensures a correct behavior of the potential in the vicinity of linear geometries. In preliminary fits the $A_0$ value was roughly optimized. The $A_1$ and $A_2$ coefficients were then determined to satisfy the above restrictions. The expansion is given explicitly in Table I. It reproduces all calculated MRCI energies to within 0.1–0.8 $cm^{-1}$. The function is expected to be valid in the geometry range $r_{OH} = 1.3$–$3.0\ a_0$ and $\phi_{HOH} = 70°$–$180°$.

In Tables II(a) and II(b) we give sets of spectroscopic constants for $H_2O^+$, $D_2O^+$, and $HDO^+$ as calculated by perturbation theory from the potential in Table I. These data are compared with available experimental data in Tables III(A) and III(B). The rotational constants in the vibrational ground state have been determined by Lew,[2] Strahan *et al.*,[7] and Dinelli *et al.*[9] from high resolution studies. The experimental $r_0$ structures deviate for each other by 0.008 Å in $r_0$ and by 1.2° in the included bond angle. These uncertainties were attributed primarily to the inertia defects.[8] Our $r_0$ structure agrees to within 0.002 Å and 0.2° with the structures of Lew[2] and Dinelli *et al.*[9] The latter authors used ex-

TABLE I. Expansion coefficients[a] of the three-dimensional near equilibrium potential energy and dipole moment surfaces of the $X$ state of $H_2O^+$ (in a.u.).

| | | | | | | | |
|---|---|---|---|---|---|---|---|
| Energy surface ($C_{ijk} = C_{jik}$)[b] | | | | | | | |
| $C_{000}$: | −75.888 455 | $C_{200}$: | 0.746 040 | $C_{110}$: | 0.006 837 | $C_{101}$: | 0.023 306 |
| $C_{002}$: | 0.030 838 | $C_{300}$: | −0.232 770 | $C_{210}$: | 0.002 530 | $C_{201}$: | 0.006 675 |
| $C_{111}$: | −0.048 878 | $C_{102}$: | −0.013 178 | $C_{003}$: | 0.003 612 | $C_{400}$: | −0.261 132 |
| $C_{310}$: | −0.005 833 | $C_{220}$: | 0.001 575 | $C_{301}$: | −0.021 047 | $C_{211}$: | −0.001 235 |
| $C_{202}$: | −0.021 059 | $C_{112}$: | 0.031 272 | $C_{103}$: | 0.003 679 | $C_{004}$: | 0.001 583 |
| $C_{500}$: | −0.077 210 | $C_{410}$: | 0.002 827 | $C_{320}$: | 0.000 963 | $C_{401}$: | −0.017 975 |
| $C_{311}$: | 0.064 680 | $C_{221}$: | 0.024 067 | $C_{302}$: | −0.021 569 | $C_{212}$: | 0.025 158 |
| $C_{203}$: | 0.008 915 | $C_{113}$: | 0.008 398 | $C_{104}$: | 0.001 161 | $C_{005}$: | 0.000 685 |
| $C_{600}$: | 0.035 389 | $C_{006}$: | 0.000 186 | | | | |
| Dipole moment surfaces[c] | | | | | | | |
| $x$ component ($C_{ijk} = C_{jik}$) | | | | | | | |
| $C_{000}$: | 0.926 844 | $C_{100}$: | 0.232 683 | $C_{001}$: | −0.515 989 | $C_{200}$: | 0.068 855 |
| $C_{110}$: | −0.104 625 | $C_{101}$: | −0.137 568 | $C_{002}$: | −0.162 010 | $C_{300}$: | −0.020 571 |
| $C_{210}$: | −0.013 804 | $C_{201}$: | −0.031 695 | $C_{111}$: | 0.027 424 | $C_{102}$: | −0.051 312 |
| $C_{003}$: | −0.033 015 | $C_{400}$: | −0.003 111 | $C_{310}$: | −0.001 267 | $C_{220}$: | 0.008 521 |
| $C_{301}$: | 0.009 801 | $C_{211}$: | 0.000 656 | $C_{202}$: | −0.012 271 | $C_{112}$: | 0.003 198 |
| $C_{103}$: | 0.039 139 | $C_{004}$: | −0.016 130 | | | | |
| $z$ component ($C_{ijk} = -C_{jik}$) | | | | | | | |
| $C_{100}$: | 0.452 678 | $C_{200}$: | 0.081 349 | $C_{101}$: | 0.336 998 | $C_{300}$: | −0.022 999 |
| $C_{210}$: | −0.036 251 | $C_{201}$: | 0.061 476 | $C_{102}$: | 0.040 254 | $C_{400}$: | −0.013 279 |
| $C_{310}$: | −0.005 525 | $C_{301}$: | −0.030 919 | $C_{211}$: | −0.002 769 | $C_{202}$: | 0.021 169 |
| $C_{103}$: | −0.017 078 | | | | | | |

[a] The calculate *ab initio* energies at particular geometries are available on request, cf. the text for the definition of the analytic expansions and coordinate system.

[b] The coordinates are $Q_1 = 1 - r_1^{ref}/r_1$, $Q_2 = 1 - r_2^{ref}/r_2$ and $Q_3 = A_0\theta + A_1\theta^2 + A_2\theta^3$ with $\theta = \varphi - \varphi^{ref}$ and $A_0 = 1.5$, $A_1 = -0.445\,65$ ($rad^{-1}$) and $A_2 = -0.091\,80$ ($rad^{-2}$). The potential has been expanded at the calculated equilibrium geometry: $r_1^{ref} = r_2^{ref} = 1.0004$ (Å), $\varphi^{ref} = 109.074°$.

[c] The coordinates are $Q_1 = r_1 - r_1^{ref}$, $Q_2 = r_2 - r_2^{ref}$ and $Q_3 = \varphi - \varphi^{ref}$. The dipole moment has been expanded at: $r_1^{ref} = r_2^{ref} = 1.0054$ (Å), $\varphi^{ref} = 110.0°$.

TABLE II. MRCI (A) rotational and (B) vibrational constants for the $X$ state of $H_2O^+$, $D_2O^+$, and $HDO^+$.

| | Constant | $H_2O^+$ | $D_2O^+$ | $HDO^+$ |
|---|---|---|---|---|
| (A) | $R_e^{OH}$ (Å) | 1.0004 | | |
| | $R_0^{OH}$ (Å) | 1.0003 | 1.0004 | |
| | $\alpha_e^{HOH}$ (deg) | 109.0745 | | |
| | $\alpha_0^{HOH}$ (deg) | 110.2197 | 109.9130 | |
| | $A_e$ ($cm^{-1}$) | 27.9561 | | |
| | $A_0$ ($cm^{-1}$) | 28.7665 | 15.8795 | 23.6639 |
| | $B_e$ ($cm^{-1}$) | 12.5971 | | |
| | $B_0$ ($cm^{-1}$) | 12.4238 | 6.2399 | 7.9545 |
| | $C_e$ ($cm^{-1}$) | 8.6841 | | |
| | $C_0$ ($cm^{-1}$) | 8.4493 | 4.3967 | 5.8306 |
| | $\kappa$ | −0.594 | −0.671 | −0.760 |
| | $\tau_{AAAA}$ (MHz) | −3559.9 | −1101.7 | −1947.6 |
| | $\tau_{BBBB}$ (MHz) | −197.9 | −49.6 | −60.5 |
| | $\tau_{CCCC}$ (MHz) | −27.5 | −7.5 | −14.2 |
| | $\tau_{AABB}$ (MHz) | 548.9 | 152.8 | 174.9 |
| | $\tau_{BBCC}$ (MHz) | −41.1 | −12.4 | −21.8 |
| | $\tau_{CCAA}$ (MHz) | −82.6 | −14.3 | −32.4 |
| | $\tau_{ABAB}$ (MHz) | −124.2 | −33.1 | −146.5 |
| First order centrifugal distortion constants[a] | | | | |
| | $D_J$ (MHz) | 23.7 | 6.1 | 8.4 |
| | $D_{JK}$ (MHz) | −101.8 | −30.3 | 20.9 |
| | $D_K$ (MHz) | 968.1 | 299.6 | 457.7 |
| | $R_6$ (MHz) | −2.2 | −0.5 | −0.5 |
| | $\delta_J$ (MHz) | 10.6 | 2.6 | 2.9 |
| $A$—reduction distortion constants[a] | | | | |
| | $\Delta_J$ (MHz) | 28.2 | 7.1 | 9.33750 |
| | $\Delta_{JK}$ (MHz) | −128.7 | −36.3 | 15.1 |
| | $\Delta_K$ (MHz) | 990.5 | 304.7 | 462.5 |
| | $\delta_J$ (MHz) | 10.6 | 2.6 | 2.9 |
| | $\delta_K$ (MHz) | 20.5 | 7.3 | 38.2 |
| (B) | $\omega_1$ ($cm^{-1}$) | 3380.6 | 2434.6 | 2477.8 |
| | $\omega_2$ ($cm^{-1}$) | 1476.6 | 1081.8 | 1294.7 |
| | $\omega_3$ ($cm^{-1}$) | 3436.3 | 2522.7 | 3409.3 |
| | $x_{11}$ ($cm^{-1}$) | −40.2 | −20.9 | −43.8 |
| | $x_{22}$ ($cm^{-1}$) | −20.0 | −10.8 | −14.6 |
| | $x_{33}$ ($cm^{-1}$) | −44.9 | −25.3 | −83.2 |
| | $x_{12}$ ($cm^{-1}$) | −20.4 | −10.3 | −13.9 |
| | $x_{13}$ ($cm^{-1}$) | −163.7 | −84.9 | −2.7 |
| | $x_{23}$ ($cm^{-1}$) | −26.5 | −13.8 | −26.2 |
| | $\gamma^b$ ($cm^{-1}$) | −83.6 | −44.8 | 1.3 |
| | $G$ (000) ($cm^{-1}$) | 4067.8 | 2978.1 | 3544.9 |
| | $\zeta_{13}^c$ | 0.0105 | 0.0718 | −0.0351 |
| | $\zeta_{23}^c$ | −1.0000 | −0.9974 | 0.8285 |
| | $\zeta_{12}^c$ | 0.0 | 0.0 | 0.5589 |
| | $\alpha_1^A$ ($cm^{-1}$) | 0.614 | 0.186 | 0.266 |
| | $\alpha_2^A$ ($cm^{-1}$) | −3.344 | −1.336 | −2.228 |
| | $\alpha_3^A$ ($cm^{-1}$) | 1.109 | 0.496 | 0.987 |
| | $\alpha_1^B$ ($cm^{-1}$) | 0.244 | 0.098 | 0.179 |
| | $\alpha_2^B$ ($cm^{-1}$) | −0.057 | −0.026 | −0.068 |
| | $\alpha_3^B$ ($cm^{-1}$) | 0.160 | 0.055 | 0.038 |
| | $\alpha_1^C$ ($cm^{-1}$) | 0.176 | 0.070 | 0.103 |
| | $\alpha_2^C$ ($cm^{-1}$) | 0.151 | 0.057 | 0.085 |
| | $\alpha_3^C$ ($cm^{-1}$) | 0.143 | 0.050 | 0.076 |

[a] Electron spin effects have been neglected.
[b] Darling–Dennison resonance parameter.
[c] Coriolis constants.

perimental rotational constants for the bending and asymmetric stretching levels, and symmetric stretching values calculated from the *ab initio* data.[21] They derived an equilibrium structure which is also quoted in Table III(A). Their set of $\alpha$ values agrees well with our values apart from the largest constant $\alpha_2^A$, the $B_e$ and $C_e$ constants exhibit deviation of 0.03 $cm^{-1}$, and the $A_e$ constant of 0.17 $cm^{-1}$ [cf. Table III(B)]. Even though we have neglected the electron spin–rotation interaction and calculated the quartic centrifugal distortion constants at the equilibrium structure, the

TABLE III. (A) Comparison of experimental and theoretical spectroscopic constants. (B) MRCI vibrational constants for the $X$ state of $H_2O^+$.

| | | $H_2O^+$ | | | | $D_2O^+$ | |
|---|---|---|---|---|---|---|---|
| (A) | Constant | This work | Experiment | | | This work | Experiment |
| | $R_e^{OH}$ (Å) | 1.0004 | 1.001[a] | | | | |
| | $R_0^{OH}$ (Å) | 1.0003 | 0.998 | 1.006[b] | 0.9988[c] | 1.0004 | 0.9987[d] |
| | $\alpha_e^{HOH}$ (deg) | 109.07 | 108.9 | | | | |
| | $\alpha_0^{HOH}$ (deg) | 110.22 | 111.0 | 109.8 | 110.46 | 109.91 | 110.17 |
| | $A_e$ ($cm^{-1}$) | 27.956 | 27.785 | | | 15.553 | |
| | $A_0$ ($cm^{-1}$) | 28.767 | 29.037 | 29.038 | 29.026 | 15.880 | 16.032 |
| | $B_e$ ($cm^{-1}$) | 12.597 | 12.604 | | | 6.304 | |
| | $B_0$ ($cm^{-1}$) | 12.424 | 12.423 | 12.416 | 12.422 | 6.240 | 6.240 |
| | $C_e$ ($cm^{-1}$) | 8.684 | 8.714 | | | 4.486 | |
| | $C_0$ ($cm^{-1}$) | 8.449 | 8.469 | 8.472 | 8.469 | 4.397 | 4.407 |
| | First order centrifugal distortion constants | | | | | | |
| | $D_J$ (MHz) | 23.7 | | 26.0 | | 6.1 | |
| | $D_{JK}$ (MHz) | − 101.8 | | − 151.21 | | − 30.3 | |
| | $D_K$ (MHz) | 968.1 | | 1348.57 | | 299.6 | |
| | $R_6$ (MHz) | − 2.2 | | | | − 0.5 | |
| | $\delta_J$ (MHz) | 10.6 | | | | 2.6 | |
| | $A$—Reduction distortion constants | | | | | | |
| | $\Delta_J$ (MHz) | 28.2 | 31.9 | | 30.0 | 7.1 | 8.2 |
| | $\Delta_{JK}$ (MHz) | − 128.7 | − 152.0 | | − 141.8 | − 36.3 | − 42.3 |
| | $\Delta_K$ (MHz) | 990.5 | 1311.6 | | 1255.2 | 304.7 | 242.8 |
| | $\delta_J$ (MHz) | 10.6 | 11.4 | | 110.9 | 2.6 | 2.8 |
| | $\delta$ (MHz) | 20.5 | 57.3 | | 59.0 | 7.3 | 41.7 |

| | | Theory | | | Experiment | | |
|---|---|---|---|---|---|---|---|
| (B) | ($cm^{-1}$) | This work | Ref. 23 | Ref. 24 | Ref. 9 | Ref. 2 | Ref. 10 |
| | $\omega_1$ | 3380.6 | 3388 | 3576 | 3216[e] | | 3270.6 |
| | $\omega_2$ | 1476.6 | 1518 | 1422 | 1390.0[e] | 1431.173 | 1433.7 |
| | $\omega_3$ | 3436.3 | 3469 | | 3456.0 | | |
| | $x_{11}$ | − 40.2 | | | | | − 65.3 |
| | $x_{22}$ | − 20.0 | | | | − 22.8 | − 24.0 |
| | $x_{33}$ | − 44.9 | | | | | |
| | $x_{12}$ | − 20.4 | | | | | − 22.0 |
| | $x_{13}$ | − 163.7 | | | | | |
| | $x_{23}$ | − 26.5 | | | | | |
| | $\alpha_1^A$ | 0.6137 | | | 0.6313 | | |
| | $\alpha_2^A$ | − 3.3436 | | | − 4.3231 | | |
| | $\alpha_3^A$ | 1.1089 | | | 1.1869 | | |
| | $\alpha_1^B$ | 0.2435 | | | 0.2778 | | |
| | $\alpha_2^B$ | − 0.0573 | | | − 0.0535 | | |
| | $\alpha_3^B$ | 0.1604 | | | 0.1370 | | |
| | $\alpha_1^C$ | 0.1755 | | | 0.1950 | | |
| | $\alpha_2^C$ | 0.1512 | | | 0.1503 | | |
| | $\alpha_3^C$ | 0.1429 | | | 0.1451 | | |

[a] Reference 9; note that the $r_0$ value in Table IV of Ref. 9 has been misprinted.
[b] Reference 7.
[c] Reference 2.
[d] Reference 3.
[e] Calculated from the force field of Ref. 9.

signs and magnitudes of these constants are in reasonable agreement with the available experimental values for the vibrational ground state of $H_2O^+$ and $D_2O^+$ [cf. Table III(A)]. Our Coriolis constants are also given in Table II(B). The Coriolis constant $\zeta_{13}$ which is very small in $H_2O^+$ (cf. also Ref. 9) increases only slightly in other isotopic species. There have been several previous attempts to characterize the potential expansion by means of harmonic and anharmonic constants [cf. Table III(B)] and force fields in internal coordinates (cf. Table IV). Since the experimental information available so far does not allow the derivation of a reliable complete quartic field, the various estimates for the harmonic frequencies deviate from our calculated $\omega$'s by up to about 100 $cm^{-1}$. The previous theoreti-

TABLE IV. Internal quartic force fields for the $X$ state of $H_2O^+$ (in aJ/Å$^n$).

| Constant | This work | Ref. 9 | Ref. 21 |
|---|---|---|---|
| $f_{rr}$ | 6.500 | 5.860 | 6.846 |
| $f_{\alpha\alpha}$ | 0.605 | 0.540 | 0.586 |
| $f_{rR}$ | 0.030 | 0.050 | 0.035 |
| $f_{r\alpha}$ | 0.152 | 0.169 | 0.130 |
| $f_{rrr}$ | −45.06 | | −47.326 |
| $f_{\alpha\alpha\alpha}$ | −0.760 | | −0.708 |
| $f_{rrR}$ | −0.038 | | −0.064 |
| $f_{rr\alpha}$ | −0.217 | | −0.231 |
| $f_{rR\alpha}$ | −0.319 | | 0 (fixed) |
| $f_{r\alpha\alpha}$ | −0.349 | | −0.361 |
| $f_{rrrr}$ | 279.5 | | |
| $f_{\alpha\alpha\alpha\alpha}$ | −0.546 | | |
| $f_{rrrR}$ | −0.106 | | |
| $f_{rrRR}$ | 0.058 | | |
| $f_{rrr\alpha}$ | −0.435 | | |
| $f_{rrR\alpha}$ | 0.622 | | |
| $f_{rr\alpha\alpha}$ | −0.180 | | |
| $f_{rR\alpha\alpha}$ | 0.803 | | |
| $f_{r\alpha\alpha\alpha}$ | 0.729 | | |

cal force fields of Fortune *et al.*[24] and Esposti *et al.*[21] also show rather large deficiencies [cf. Table III(b)]. Our MRCI potential is much more reliable as demonstrated from the comparison of the vibrational band origins for $H_2O^+$ and $D_2O^+$ in Table V(A) and V(B). In these tables, we have also compared the variational results with the results calculated by perturbation theory which include the Darling–Dennison correction. It can be seen that the theoretical variational values agree with the available experimental data to within a few wave numbers. This strongly suggests that our calculated force fields are essentially accurate, and implies, for instance, that the anharmonic constant $x_{11}$ derived recently from the photoelectron spectra by Reutt *et al.*[10] [cf. Table III(B)] is not correct. Similarly, the harmonic frequencies $\omega_2$ obtained from the bending levels by Lew[2] [cf. Table III(B)] for $H_2O^+$ and $D_2O^+$ are too low by about 45 cm$^{-1}$ ($H_2O^+$) and 25 cm$^{-1}$ ($D_2O^+$). Also the force constants in internal coordinates calculated by Dinelli *et al.*[9] (cf. Table V) represent only a simplified approximation of the potential expansion. It will be shown in Sec. V that the MRCI potential for the electronic ground state of the water cation also reproduces the rovibrational transition energies to high accuracy. Hence, the three dimensional analytic potential energy function in Table I represents the best compact characterization of the $H_2O^+$ electronic ground state to date.

## IV. ELECTRIC DIPOLE MOMENT FUNCTION OF $H_2O^+$ AND VIBRATIONAL BAND INTENSITIES

The dipole moments for the 50 symmetry unique geometries in the vicinity of the equilibrium geometry were first transformed to the center of mass and then fitted by a quartic expansion in the displacement coordinates $Q_1$, $Q_2 = r - r_{\rm ref}$, $Q_3 = \phi - \phi_{\rm ref}$. Then the functions were rotated into a coordinate system used in the nuclear motion Hamiltonian (the molecule lies in the $xz$ plane, the origin coincides with the oxygen atom and the positive $x$ axis bisects the angle included by the OH bonds for all geometries; the $z$ axis is perpendicular to the $x$ axis and the $H_1$ atom lies in the positive $xz$ quadrant). Both $x$ and $z$ components of the dipole moment in this coordinate system are given explicitly in Table I. The electric dipole moments in the vibrational ground states have been calculated to be 2.398 D ($H_2O^+$) and 2.139 D

TABLE V. (A) Vibrational band origins, vibrational band intensities (at 300 K) and radiative lifetime for the $X$ state of $H_2O^+$. (B) Vibrational band origins, vibrational absorption intensities (at 300 K) and radiative lifetimes for the $X$ state of $D_2O^+$.

| | $v_1$ | $v_2$ | $v_3$ | Pert[a] (cm$^{-1}$) | Var.[b] (cm$^{-1}$) | Obs.[c] (cm$^{-1}$) | $S$[d] (atm$^{-1}$ cm$^{-2}$) | $t$[e] (ms) |
|---|---|---|---|---|---|---|---|---|
| (A) | 0 | 1 | 0 | 1413.1 | 1410.4 | 1408.404 | 0.7017 + 03 | 23.4 |
| | 0 | 2 | 0 | 2786.2 | 2774.2 | 2771.271 | 0.4726 + 01 | 12.0 |
| | 1 | 0 | 0 | 3208.1 | 3211.0 | 3213.00 | 0.4452 + 03 | 7.0 |
| | 0 | 0 | 1 | 3251.3 | 3255.0 | 3259.031 | 0.1719 + 04 | 1.8 |
| | 0 | 3 | 0 | 4119.2 | 4083.6 | 4085. | 0.3482 − 01 | 8.3 |
| | 1 | 1 | 0 | 4600.9 | 4600.1 | 4593. | 0.1806 + 00 | 5.7 |
| | 0 | 1 | 1 | 4637.9 | 4639.9 | | 0.5739 + 02 | 1.5 |
| | 0 | 4 | 0 | 5412.1 | 5323.4 | | 0.1240 − 02 | 6.7 |
| | 1 | 2 | 0 | 5953.6 | 5942.3 | 5936 | 0.1392 − 01 | 4.9 |
| | 0 | 2 | 1 | 5984.5 | 5980.8 | | 0.3424 + 00 | 1.3 |
| | 2 | 0 | 0 | 6282.2 | 6296.7 | 6298 | 0.4711 + 01 | 2.2 |
| | 1 | 0 | 1 | 6295.8 | 6310.2 | | 0.2660 + 02 | 1.5 |
| | 0 | 0 | 2 | 6466.2 | 6475.0 | | 0.8388 + 00 | 1.2 |
| | 0 | 5 | 0 | 6665.0 | 6462.9 | | 0.4380 − 03 | 6.0 |
| | 1 | 3 | 0 | 7266.2 | 7228.6 | 7234 | 0.2683 − 02 | 4.3 |
| | 0 | 3 | 1 | 7291.0 | 7271.2 | | 0.3691 − 02 | 1.1 |
| | 2 | 1 | 0 | 7650.9 | 7662.2 | 7639 | 0.1859 − 02 | 1.9 |
| | 1 | 1 | 1 | 7662.0 | 7672.9 | | 0.1645 + 01 | 1.3 |
| | 0 | 1 | 2 | 7830.1 | 7837.3 | | 0.9107 − 02 | 1.1 |
| | 0 | 6 | 0 | 7877.8 | 7496.6 | | 0.4502 − 04 | 5.7 |

TABLE V (*continued*).

| | $v_1$ | $v_2$ | $v_3$ | Pert[a] ($cm^{-1}$) | Var.[b] ($cm^{-1}$) | Obs.[c] ($cm^{-1}$) | $S$[d] ($atm^{-1}\,cm^{-2}$) | $t$[e] (ms) |
|---|---|---|---|---|---|---|---|---|
| (B) | 0 | 1 | 0 | 1048.1 | 1047.04 | 1044.27 | 0.27359 + 03 | 108.8 |
| | 0 | 2 | 0 | 2074.5 | 2070.21 | 2063 | 0.33977 + 01 | 54.5 |
| | 1 | 0 | 0 | 2345.2 | 2346.17 | 2342 | 0.21189 + 03 | 27.6 |
| | 0 | 0 | 1 | 2422.7 | 2424.20 | | 0.77816 + 03 | 7.1 |
| | 0 | 3 | 0 | 3079.2 | 3067.51 | 3058.66 | 0.12260 − 01 | 36.8 |
| | 1 | 1 | 0 | 3383.0 | 3382.21 | 3373 | 0.13172 + 00 | 23.1 |
| | 0 | 1 | 1 | 3457.0 | 3457.77 | | 0.21212 + 02 | 6.2 |
| | 0 | 4 | 0 | 4062.2 | 4035.79 | | 0.46914 − 03 | 28.1 |
| | 1 | 2 | 0 | 4399.1 | 4393.58 | 4396 | 0.23590 − 01 | 19.7 |
| | 0 | 2 | 1 | 4469.6 | 4468.37 | | 0.21381 + 00 | 5.4 |
| | 2 | 0 | 0 | 4636.0 | 4640.66 | 4638 | 0.16084 + 01 | 12.3 |
| | 1 | 0 | 1 | 4683.1 | 4688.47 | | 0.97678 + 01 | 5.8 |
| | 0 | 0 | 2 | 4807.5 | 4812.45 | | 0.10768 + 00 | 3.9 |
| | 0 | 5 | 0 | 5023.5 | 4970.48 | | 0.18158 − 05 | 23.3 |
| | 1 | 3 | 0 | 5393.5 | 5378.54 | | 0.25269 − 03 | 17.3 |
| | 0 | 3 | 1 | 5460.5 | 5454.37 | | 0.39552 − 02 | 4.9 |
| | 2 | 1 | 0 | 5662.9 | 5666.09 | 5650 | 0.39225 − 02 | 11.1 |
| | 1 | 1 | 1 | 5707.1 | 5710.75 | | 0.43089 + 00 | 5.3 |
| | 0 | 1 | 2 | 5828.5 | 5833.32 | | 0.87724 − 03 | 3.5 |
| | 0 | 6 | 0 | 5963.2 | 5874.59 | | 0.57745 − 06 | 19.8 |
| | 1 | 4 | 0 | 6366.3 | 6333.82 | | 0.31524 − 07 | 15.5 |
| | 0 | 4 | 1 | 6429.7 | 6413.13 | | 0.49941 − 04 | 4.4 |
| | 2 | 2 | 0 | 6668.2 | 6666.02 | 6694 | 0.61186 − 03 | 10.2 |
| | 1 | 2 | 1 | 6709.4 | 6709.02 | | 0.59615 − 02 | 4.8 |
| | 0 | 2 | 2 | 6827.9 | 6831.97 | | 0.30316 − 05 | 3.2 |
| | 3 | 0 | 0 | 6857.0 | 6877.37 | 6860 | 0.59124 − 02 | 6.1 |
| | 2 | 0 | 1 | 6876.5 | 6891.42 | | 0.21228 + 00 | 4.7 |
| | 0 | 7 | 0 | 6881.1 | 6789.56 | | 0.61582 − 06 | 16.8 |
| | 1 | 0 | 2 | 7023.5 | 7054.30 | | 0.12277 − 01 | 4.2 |
| | 0 | 0 | 3 | 7141.6 | 7152.85 | | 0.22507 − 01 | 2.7 |
| | 1 | 5 | 0 | 7317.3 | 7255.99 | | 0.49840 − 06 | 14.3 |
| | 0 | 5 | 1 | 7377.2 | 7342.11 | | 0.16158 − 05 | 3.9 |
| | 2 | 3 | 0 | 7651.7 | 7640.68 | | 0.35502 − 04 | 9.4 |
| | 1 | 3 | 1 | 7690.0 | 7682.33 | | 0.24775 − 03 | 4.4 |

[a] Calculated from the spectroscopic constant of Table II.
[b] Calculated variationally for $J = 0$.
[c] References 2, 3, 7, and 10.
[d] $S$ (at 300 K in $cm^{-2}\,atm^{-1}$) $= 10.25 \times \Delta E(cm^{-1}) \times R^2(D^2)$; 0.7017 + 03 signifies $0.7017 \times 10^3$.
[e] $\tau_i = 1/\Sigma_{ij} A$; $A_{ij}(s^{-1}) = 3.2043 \times 10^{-7} \times \Delta E^3(cm^{-1}) \times R^2(D^2)$.

($D_2O^+$) with the center of mass as origin, i.e., larger than in neutral $H_2O$ (1.855 D[41]). Esposti *et al.*[21] calculated the SCF value of the $H_2O^+$ dipole moment with the center of mass as origin to be 2.60 D and estimated that this value is too large by about 0.3 D, in accord with the present result. We have transformed the dipole functions into Eckart frame internal coordinates and, by applying the *l*-tensor algebra, into dimensionless normal coordinates. The linear and quadratic terms of this expansion are given in Table VI. The expansion coefficients show that the electric dipole moment function of the water cation can be well approximated by its linear form for lower vibrational states, since all the quadratic terms are rather small. For the electronic ground state of neutral water[38] the linear terms are: $\mu_1' = -0.0217$ D, $\mu_2' = 0.1795$ D, and $\mu_3' = 0.0988$ D. Hence, for the symmetric stretching mode in $H_2O^+$ the linear term of the *b*-component dipole has been calculated to be about 3 times larger than in $H_2O$. For the bending mode it is somewhat smaller, whereas for the asymmetric mode it is about the same in both species. Accordingly, the fundamental transitions in $H_2O$ exhibit vibrational band intensities $\nu_2 > \nu_3 > \nu_1$, whereas the $H_2O^+$ the ordering is calculated to be $\nu_3 > \nu_2 > \nu_1$. In Tables VII(A)

TABLE VI. First and second derivatives of the Eckart frame[a] dipole moment for the $X$ state of $H_2O^+$ with respect to dimensionless normal coordinates (in debye).

| | | | | | |
|---|---|---|---|---|---|
| | *a* component | | | | |
| $\mu_1'$ | 0.0 | $\mu_{11}''$ | 0.0 | $\mu_{12}''$ | − 0.0126 |
| $\mu_2'$ | 0.0 | $\mu_{22}''$ | 0.0 | $\mu_{13}''$ | 0.0 |
| $\mu_3'$ | − 0.1260 | $\mu_{33}''$ | 0.0 | $\mu_{23}''$ | − 0.0058 |
| | *b* component | | | | |
| $\mu_1'$ | 0.0644 | $\mu_{11}''$ | 0.0013 | $\mu_{11}''$ | − 0.0001 |
| $\mu_2'$ | − 0.1169 | $\mu_{22}''$ | − 0.0048 | $\mu_{13}''$ | 0.0 |
| $\mu_3'$ | 0.0 | $\mu_{33}''$ | 0.0088 | $\mu_{23}''$ | 0.0 |

[a] The Eckart system is defined with respect to the molecular fixed axes *a*, *b*, and *c*.

TABLE VII. Dipole matrix elements[a] (in D, lower triangle and diagonal elements) and rates of spontaneous emission ($s^{-1}$) (upper triangle) between the low lying vibrational states of (A) $H_2O^+$ and (B) $D_2O^+$.

| | Mode | 000 | 010 | 020 | 100 | 001 | 030 | 110 | 011 | 040 | 120 |
|---|---|---|---|---|---|---|---|---|---|---|---|
| (A) | 000 | 2.398 + 0 | 0.4273 + 2 | 0.1113 + 1 | 0.1401 + 3 | 0.5557 + 3 | 0.1777 − 1 | 0.1170 + 0 | 0.3782 + 2 | 0.1076 − 2 | 0.3451 − 1 |
| | 010 | 2.204 − 1 | 2.345 + 0 | 0.8224 + 2 | 0.2663 + 1 | 0.4602 + 0 | 0.1988 + 1 | 0.1270 + 3 | 0.5762 + 3 | 0.6788 − 1 | 0.2048 + 0 |
| | 020 | 1.289 − 2 | 3.215 − 1 | 2.280 + 0 | 0.2211 − 2 | 0.9611 − 3 | 0.1182 + 3 | 0.4570 + 1 | 0.8206 + 0 | 0.1784 + 1 | 0.1153 + 3 |
| | 100 | 1.163 − 1 | 3.823 − 2 | 9.289 − 3 | 2.445 + 0 | 0.2038 − 3 | 0.7605 − 2 | 0.4333 + 2 | 0.2114 + 0 | 0.8075 − 3 | 0.1456 + 1 |
| | 001 | 2.270 − 1 | 1.533 − 2 | 5.312 − 3 | 8.977 − 2 | 2.473 + 0 | 0.1593 − 3 | 0.1643 − 1 | 0.4175 + 2 | 0.3821 − 5 | 0.3437 − 1 |
| | 030 | 9.121 − 4 | 4.630 − 2 | 4.097 − 1 | 6.011 − 3 | 9.386 − 4 | 2.196 + 0 | 0.1224 − 1 | 0.3581 − 2 | 0.1482 + 3 | 0.5903 + 1 |
| | 110 | 1.958 − 3 | 1.117 − 1 | 4.893 − 2 | 2.263 − 1 | 4.621 − 3 | 1.683 − 2 | 2.391 + 0 | 0.1696 − 3 | 0.2213 − 1 | 0.8178 + 2 |
| | 011 | 3.474 − 2 | 2.335 − 1 | 2.007 − 2 | 1.515 − 2 | 2.230 − 1 | 8.143 − 3 | 9.262 − 2 | 2.421 + 0 | 0.4248 − 3 | 0.2735 − 1 |
| | 040 | 1.508 − 4 | 1.901 − 3 | 1.853 − 2 | 5.215 − 4 | 3.701 − 5 | 4.979 − 1 | 1.366 − 2 | 2.059 − 3 | 2.074 + 0 | 0.6917 − 1 |
| | 120 | 7.241 − 4 | 2.648 − 3 | 1.075 − 1 | 1.507 − 2 | 2.371 − 3 | 5.414 − 2 | 3.284 − 1 | 6.283 − 3 | 3.050 − 2 | 2.327 + 0 |
| (B) | 000 | 2.140 + 0 | 0.9181 + 1 | 0.4460 + 0 | 0.3573 + 2 | 0.1401 + 3 | 0.3533 − 2 | 0.4615 − 1 | 0.7768 + 1 | 0.2340 − 3 | 0.1395 − 1 |
| | 010 | 1.597 − 1 | 2.107 + 0 | 0.1790 + 2 | 0.5493 + 0 | 0.1154 + 0 | 0.9950 + 0 | 0.3296 + 2 | 0.1441 + 3 | 0.1303 − 1 | 0.8166 − 1 |
| | 020 | 1.266 − 2 | 2.308 − 1 | 2.070 + 0 | 0.3243 − 3 | 0.2860 − 3 | 0.2621 + 2 | 0.9488 + 0 | 0.2045 + 0 | 0.1425 + 1 | 0.3067 + 2 |
| | 100 | 9.391 − 2 | 2.826 − 2 | 7.015 − 3 | 2.167 + 0 | 0.5161 − 3 | 0.1419 − 2 | 0.9391 + 1 | 0.4805 − 1 | 0.2309 − 5 | 0.5449 + 0 |
| | 001 | 1.770 − 1 | 1.187 − 2 | 4.534 − 3 | 5.884 − 2 | 2.190 + 0 | 0.1698 − 4 | 0.1430 − 2 | 0.8930 + 1 | 0.2821 − 5 | 0.1144 − 1 |
| | 030 | 6.247 − 4 | 1.961 − 2 | 2.902 − 1 | 3.472 − 3 | 4.509 − 4 | 2.026 + 0 | 0.1394 − 2 | 0.9625 − 3 | 0.3407 + 2 | 0.1257 + 1 |
| | 110 | 1.950 − 3 | 9.084 − 2 | 3.660 − 2 | 1.641 − 1 | 2.277 − 3 | 1.194 − 2 | 2.134 + 0 | 0.4893 − 3 | 0.4272 − 2 | 0.1808 + 2 |
| | 011 | 2.448 − 2 | 1.811 − 1 | 1.562 − 2 | 1.056 − 2 | 1.606 − 1 | 7.185 − 3 | 6.013 − 2 | 2.159 + 0 | 0.5023 − 4 | 0.2158 − 2 |
| | 040 | 1.065 − 4 | 1.247 − 3 | 2.446 − 2 | 3.906 − 5 | 4.636 − 5 | 3.459 − 1 | 6.984 − 3 | 9.106 − 4 | 1.974 + 0 | 0.4341 − 2 |
| | 120 | 7.241 − 4 | 2.636 − 3 | 8.829 − 2 | 1.423 − 2 | 2.185 − 3 | 4.145 − 2 | 2.360 − 1 | 2.897 − 3 | 1.738 − 2 | 2.097 + 0 |

[a] Absolute values of the total dipole matrix elements are given, 2.398 + 0 signifies $2.398 \times 10^0$.

and VII(B) rotationless dipole moment matrix elements and Einstein coefficients of spontaneous emission for low lying vibrational states of $H_2O^+$ and $D_2O^+$ are given. These data have been used in the evaluation of the vibrational band intensities for absorption from the vibrational ground state into higher overtones and for the calculations of the radiative lifetimes [cf. Table V(A) and V(B)]. In Table VIII we compare some vibrational ground state band intensities for absorption (at 300 K), calculated from rotationless transition dipole matrix elements [cf. footnote in Table V(A) for definition] with the integrated band intensities, calculated from the sums of all line intensities (at 300 K, up to $J'' = 9$, cf. Sec. V). For the symmetric stretching mode the agreement is excellent, but for the bending and the asymmetric stretching modes both sets are not completely equivalent because of the Coriolis interactions between these modes. In this case the vibration–rotation coupling complicates the definition of the rotationless dipole matrix elements and the integrated band intensities are seen to be more accurate.

All lifetimes for vibrationally excited states of $H_2O^+$ lie on the millisecond time scale and decrease with increasing vibrational quantum numbers. In $D_2O^+$ the lifetimes are longer, mainly because of the smaller energy gaps between the vibrational levels. In both species the lifetimes vary in a mode specific way, i.e., they decrease with increasing quantum number of a given mode in pure overtones or combination levels, Recently, the radiative lifetimes of vibrational levels in molecular ions became experimentally accessible by monitoring the excited state decay via fast ion–molecule reactions.[42]

TABLE VIII. Vibrational and integrated band intensities $S_v$ and $S_i$ of the $X$ state for $H_2O^+$ ($atm^{-1}\,cm^{-2}$) at 300 K.

| Transition | $S_v$[a] | $S_i$[b] |
|---|---|---|
| 010–000 | 701.7 | 634.2 |
| 020–000 | 4.73 | 5.27 |
| 100–000 | 445.2 | 445.8 |
| 001–000 | 1719.0 | 1693.0 |
| 030–000 | 0.035 | 0.024 |

[a] Footnote of Table V for definition.
[b] Calculated as a sum of $S_i$ values up to $J'' = 9$.

## V. ROVIBRATIONAL ABSORPTION SPECTRUM OF $H_2O^+$

Using the variational procedure described previously, we have calculated the energies of the rovibrational levels in $H_2O^+$ and the dipole transition matrix elements for transitions between such levels. Our calculations were performed for all vibrational levels up to 8000 $cm^{-1}$ above the ground state levels and included all rotational levels up to $J = 9$. In this paper, we present only that portion of the results which corresponds to the purely rotational absorption spectrum of $H_2O^+$ and to the rovibrational transitions from the vibrational ground state levels to the $\nu_2$, $2\nu_2$, $3\nu_2$, $\nu_1$, and $\nu_3$ levels. From the dipole transition matrix elements the individual line intensities were calculated from the usual formula[43]

$$S_i = 3054.6\, g_{NS}\, \nu_i R^2 \exp(-E_r/kT) \times [1 - \exp(-\nu_i/kT)]/(T Q_r),$$

where $S_i$ in $cm^{-2}\,atm^{-1}$, is the line intensity at temperature $T$, $g_{NS}$ is the nuclear spin statistical weight (1 or 3), $\nu_i$ is the transition frequency in $cm^{-1}$, $R^2$ is the squared transition dipole matrix element in $D^2$ (which already includes effects

usually accounted for by Hönl–London and Hermann–Wallis factors for symmetric rotors and also the $2J + 1$ degeneracy factor, because we are essentially calculating $R^2$ exactly), $E_r$ is the energy, in $cm^{-1}$, of the rotational level in the vibrational ground state, $k$ is the Boltzmann constant ($k = 0.6950\ cm^{-1}/K$) and $T$ is the absolute temperature, which has been taken to be 300 K. The rotational partition function $Q_r = \Sigma\, g_{NS}\,(2J + 1)\exp(-E_r/kT)$ was evaluated from the variationally calculated rotational levels up to $J'' = 9$. Its value equals 198.04. An independent approximate expression[44]

$$Q_r = 2[\pi(kT)^3/ABC]^{1/2},$$

where $A_e$, $B_e$, and $C_e$ are the rotational constants [cf. Table II(A)] yields 193.0. In the calculations of line intensities the value obtained from the variationally calculated rotational levels was used. The contributions of the vibrational partition function have been neglected, since they would not significantly change the results at 300 K. In Figs. 1–6 the absorption spectra of $H_2O^+$ at 300 K are displayed. So far, such complete spectra are experimentally not accessible, as usual, only portions of the rovibrational transitions can be measured by laser spectroscopy. In Table IX the transition energies (in $cm^{-1}$), the absolute line intensities $S_i$ (in $atm^{-1}\ cm^{-2}$ at 300 K) and the squares of the electric dipole transition matrix elements (in a.u.$^2$) are given for some intense transitions within the $P$, $Q$, and $R$ branches in the vibrational ground state and for the $\nu_2$, $2\nu_2$, $\nu_1$, $\nu_3$, and $3\nu_2$ rovibrational transitions. The accuracy of our potential energy function and the variational method used in the calculation of rovibrational energy levels can be checked by comparison of the purely *ab initio* calculated data with available experiments. In the experimental spectra the rovibrational states are split into two states because of the electron spin–rotation coupling effects. In the rovibrational levels of $H_2O^+$ such $F_1$ and $F_2$ components are often split[7,9,19] by as much as 1.0 $cm^{-1}$. Since in our treatment such coupling effects have been neglected, we use the quantum number $J$ instead of $N$ and the arithmetic mean values of the corresponding experimental doublets for comparison (cf. Table X). In the vibrational ground state the combination differences of the rotational levels agree to within 0.01–0.5 $cm^{-1}$ with the data of Dinelli *et al.*,[9] the transition energies for $\nu_2$ to within 1.5 to 3.0 $cm^{-1}$ with the values of Stickland and Davies[19] and for $\nu_3$ to within 3–4 $cm^{-1}$ with the values of Dinelli *et al.*[9] To date, there have been no absolute exprimental intensity measurements. Lew,[2,3] however, has estimated the line intensity patterns for some rotational and rovibrational bands in $H_2O^+$ and $D_2O^+$. His data are compared with our squared dipole transition matrix elements in Table XI. Even though the absolute values differ considerably, the relative intensities within a given band are in satisfactory agreement. The presented absolute values of the rovibrational transition dipole matrix element and absolute line intensities are expected to prove useful in the determination of the abundance of $H_2O^+$ in outer space and under laboratory conditions.

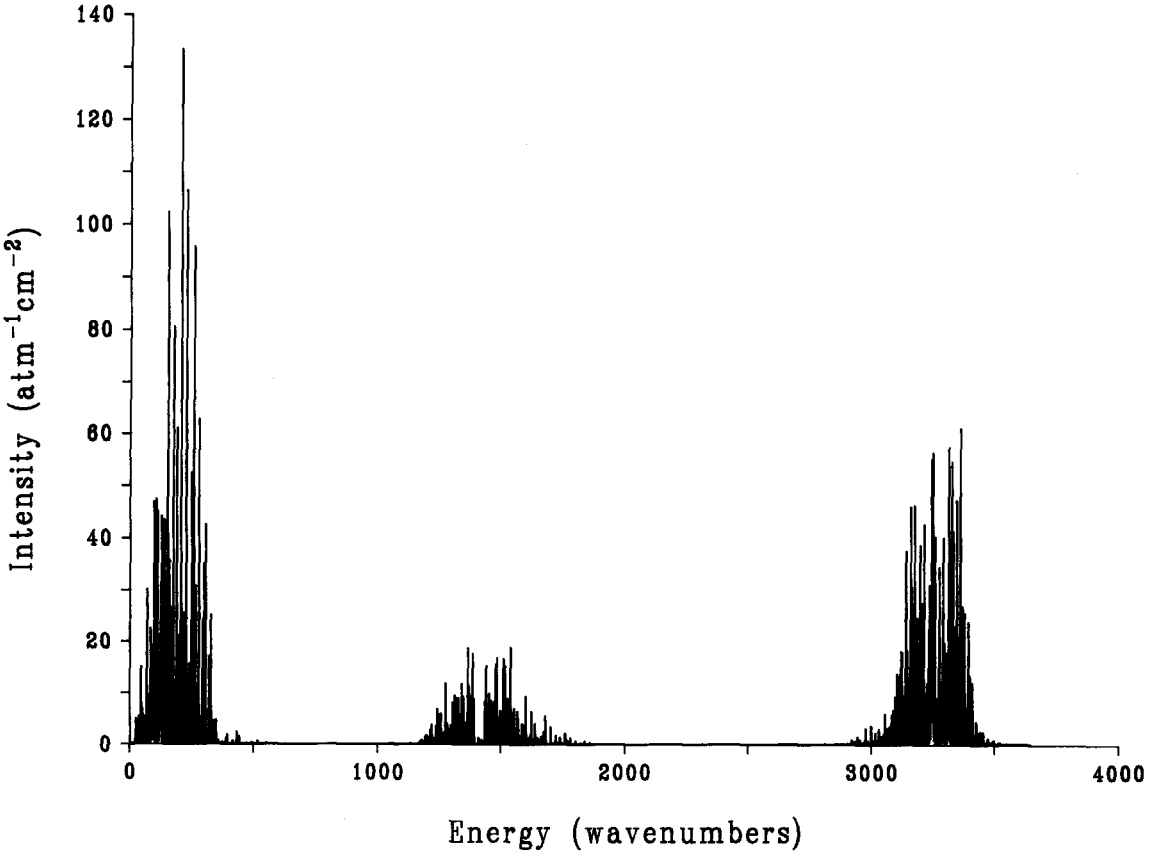


FIG. 1. Theoretical rovibrational absorption spectrum of the $H_2O^+$ ion between 0 and 4000 $cm^{-1}$ (at 300 K). Gaussian HWHM's were chosen for each single transition to be 1 $cm^{-1}$.

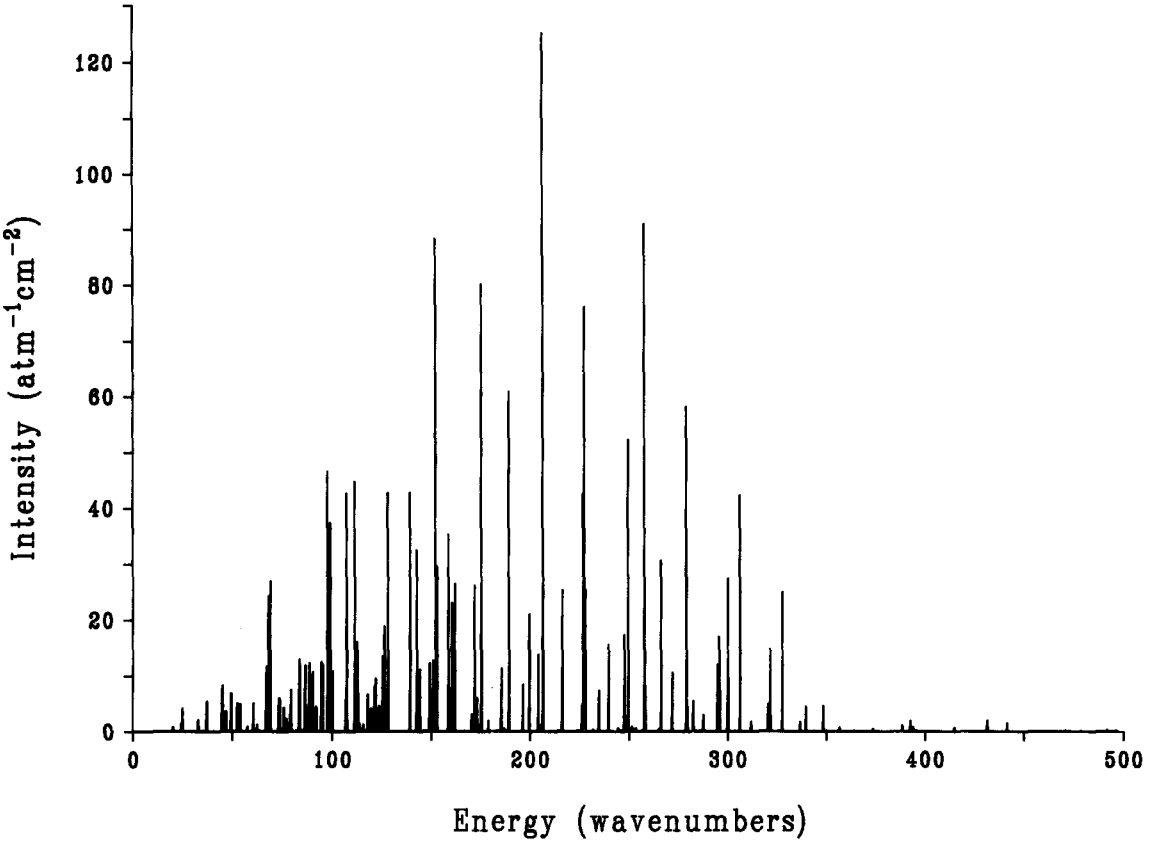


FIG. 2. Theoretical rotational absorption spectrum in the vibrational ground state of the $H_2O^+$ ion (at 300 K) with HWHM = 0.1 cm$^{-1}$.

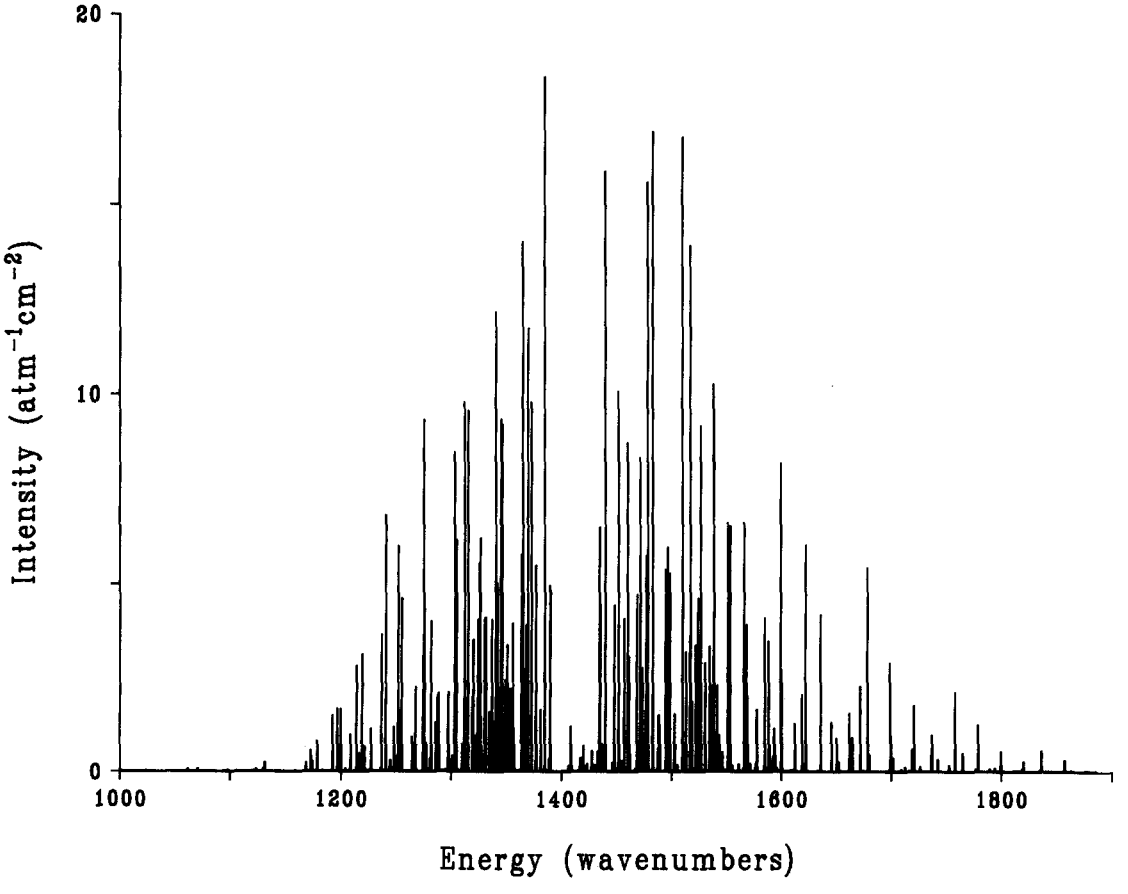


FIG. 3. Theoretical rovibrational absorption spectrum of the $\nu_2$ transition of the $H_2O^+$ ion (at 300 K) with HWHM = 0.2 cm$^{-1}$.

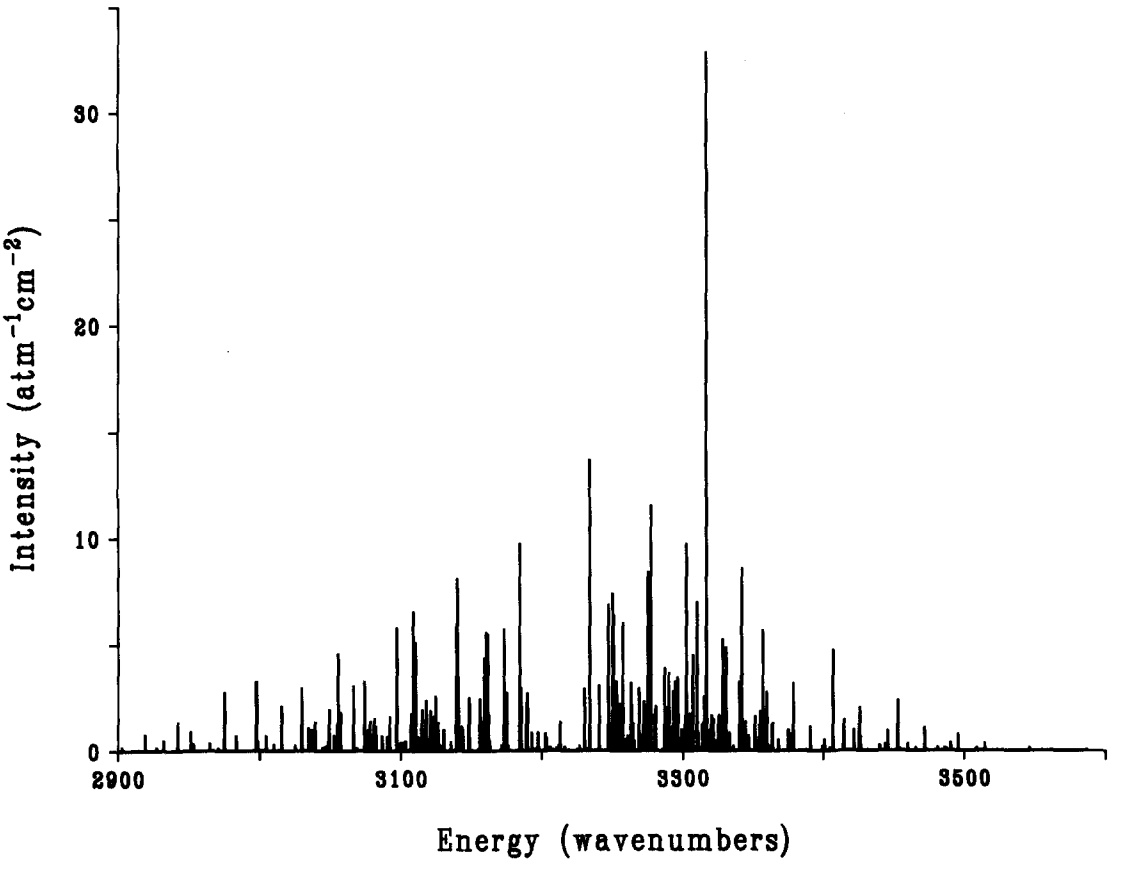


FIG. 4. Theoretical rovibrational absorption spectrum of the $\nu_1$ transition of the $H_2O^+$ ion (at 300 K) with HWHM = 0.2 cm$^{-1}$.

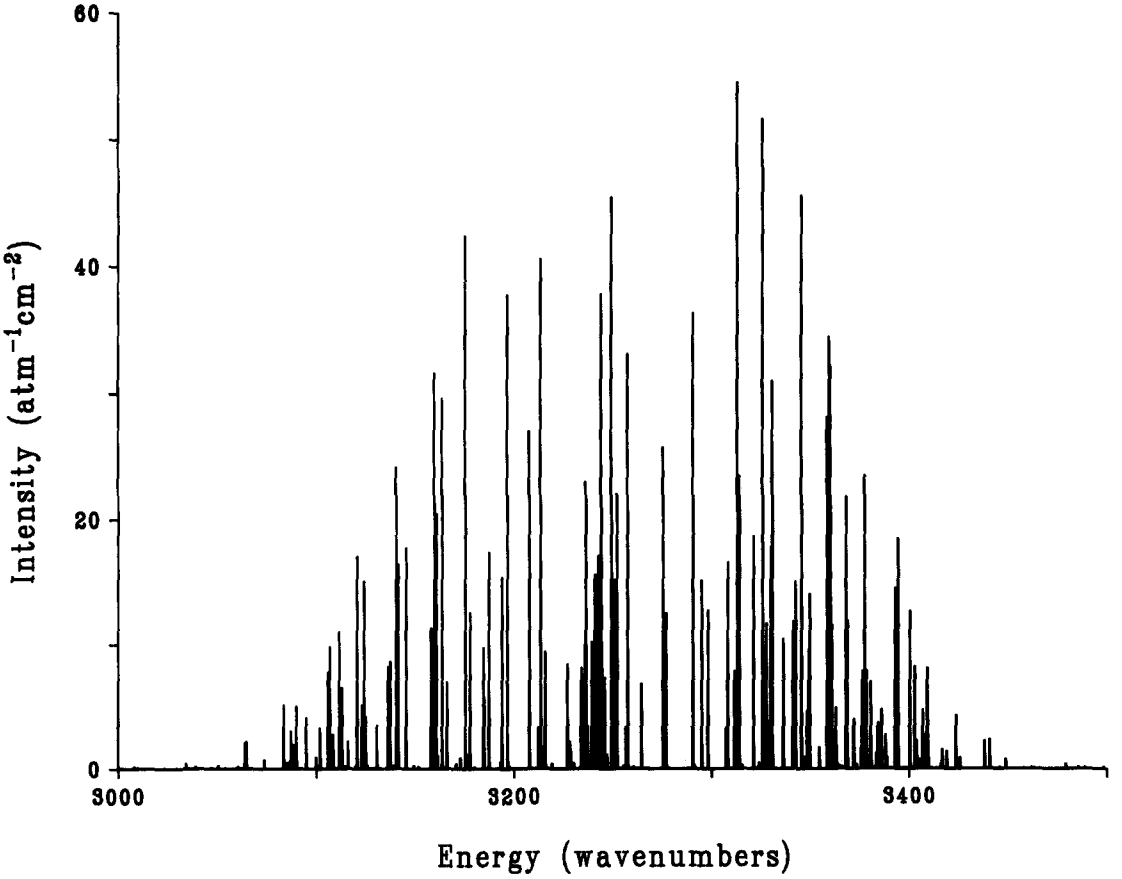


FIG. 5. Theoretical rovibrational absorption spectrum of the $\nu_3$ transition of the $H_2O^+$ ion (at 300 K) with HWHM = 0.2 cm$^{-1}$.

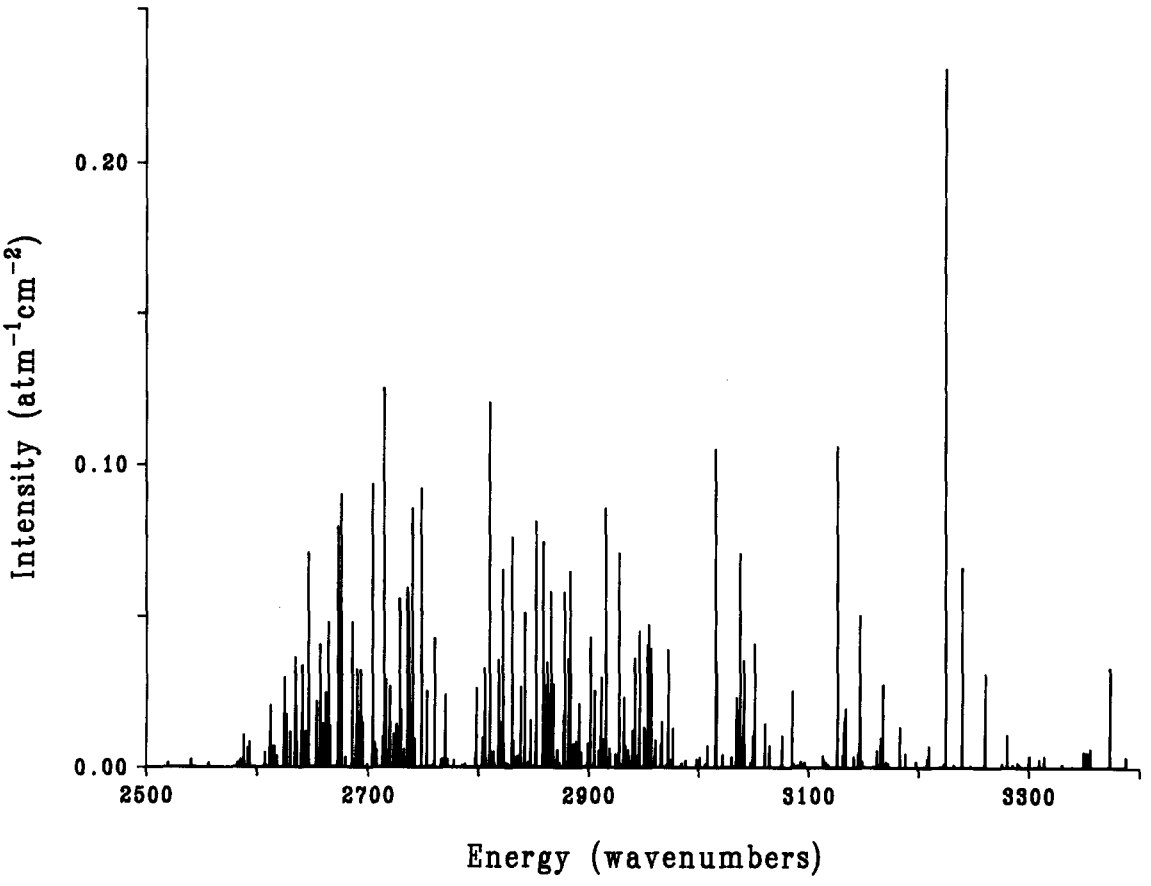


FIG. 6. Theoretical rovibrational absorption spectrum of the $2\nu_2$ transition of the $H_2O^+$ ion (at 300 K) with HWHM = 0.2 cm$^{-1}$.

TABLE IX. Variationally calculated rovibrational absorption line intensities[a] (at 300 k) for the $X$ state of $H_2O^+$.

| $J'$ | $K'_a$ | $K'_c$ | $J''$ | $K''_a$ | $K''_c$ | $\Delta E$(cm$^{-1}$) | $S$(atm$^{-1}$ cm$^{-2}$) | $R^2$(a.u.$^2$) |
|---|---|---|---|---|---|---|---|---|
| Vibrational transition 000–000 | | | | | | | | |
| *P* branch | | | | | | | | |
| 6 | 3 | 4 | 7 | 0 | 7 | 73.89 | 0.130 − 01 | 0.228 − 01 |
| 5 | 3 | 3 | 6 | 0 | 6 | 74.39 | 0.529 − 01 | 0.166 − 01 |
| 7 | 3 | 5 | 8 | 0 | 8 | 77.46 | 0.245 − 01 | 0.263 − 01 |
| *Q* branch | | | | | | | | |
| 4 | 2 | 2 | 4 | 1 | 3 | 45.34 | 0.831 + 01 | 0.304 + 01 |
| 3 | 2 | 2 | 3 | 1 | 3 | 67.32 | 0.118 + 02 | 0.120 + 01 |
| 4 | 3 | 1 | 4 | 2 | 2 | 84.02 | 0.118 + 02 | 0.171 + 01 |
| *R* branch | | | | | | | | |
| 5 | 1 | 5 | 4 | 0 | 4 | 97.91 | 0.471 + 02 | 0.336 + 01 |
| 3 | 2 | 2 | 2 | 1 | 1 | 111.63 | 0.453 + 02 | 0.149 + 01 |
| 3 | 3 | 1 | 2 | 2 | 1 | 152.38 | 0.895 + 02 | 0.219 + 01 |
| Vibrational transition 010–000 | | | | | | | | |
| *P* branch | | | | | | | | |
| 2 | 2 | 0 | 3 | 3 | 1 | 1275.17 | 0.903 + 01 | 0.285 − 01 |
| 2 | 1 | 1 | 3 | 2 | 2 | 1303.29 | 0.820 + 01 | 0.164 − 01 |
| 5 | 1 | 5 | 6 | 0 | 6 | 1304.84 | 0.597 + 01 | 0.321 − 01 |
| *Q* branch | | | | | | | | |
| 4 | 0 | 4 | 4 | 1 | 3 | 1365.15 | 0.115 + 02 | 0.274 − 01 |
| 2 | 1 | 1 | 2 | 2 | 0 | 1365.30 | 0.763 + 01 | 0.108 − 01 |
| 4 | 1 | 3 | 4 | 2 | 2 | 1369.86 | 0.114 + 02 | 0.336 − 01 |

TABLE IX (*continued*).

| $J'$ | $K'_a$ | $K'_c$ | $J''$ | $K''_a$ | $K''_c$ | $\Delta E(\text{cm}^{-1})$ | $S(\text{atm}^{-1}\,\text{cm}^{-2})$ | $R^2(\text{a.u.}^2)$ |
|---|---|---|---|---|---|---|---|---|
| *R* branch | | | | | | | | |
| 4 | 0 | 4 | 3 | 1 | 3 | 1478.62 | 0.152 + 02 | 0.193 − 01 |
| 3 | 1 | 3 | 2 | 0 | 2 | 1483.20 | 0.164 + 02 | 0.149 − 01 |
| 5 | 1 | 5 | 4 | 0 | 4 | 1510.28 | 0.163 + 02 | 0.282 − 01 |
| Vibrational transition 020–000 | | | | | | | | |
| *P* branch | | | | | | | | |
| 6 | 0 | 6 | 7 | 1 | 7 | 2646.31 | 0.561 − 01 | 0.275 − 03 |
| 5 | 1 | 5 | 6 | 0 | 6 | 2673.16 | 0.821 − 01 | 0.215 − 03 |
| 2 | 1 | 1 | 3 | 2 | 2 | 2673.89 | 0.518 − 01 | 0.504 − 04 |
| *Q* branch | | | | | | | | |
| 2 | 0 | 2 | 2 | 1 | 1 | 2748.64 | 0.950 − 01 | 0.527 − 04 |
| 2 | 1 | 1 | 2 | 0 | 2 | 2810.62 | 0.125 + 00 | 0.600 − 04 |
| 4 | 1 | 3 | 4 | 0 | 4 | 2830.94 | 0.783 − 01 | 0.724 − 04 |
| *R* branch | | | | | | | | |
| 3 | 1 | 3 | 2 | 0 | 2 | 2852.77 | 0.837 − 01 | 0.396 − 04 |
| 2 | 2 | 0 | 1 | 1 | 1 | 2915.95 | 0.878 − 01 | 0.362 − 04 |
| 3 | 2 | 2 | 2 | 1 | 1 | 2927.93 | 0.733 − 01 | 0.382 − 04 |
| Vibrational transition 100–000 | | | | | | | | |
| *P* branch | | | | | | | | |
| 2 | 2 | 0 | 3 | 3 | 1 | 3055.71 | 0.463 + 01 | 0.609 − 02 |
| 5 | 1 | 5 | 6 | 0 | 6 | 3097.40 | 0.445 + 01 | 0.101 − 01 |
| 2 | 1 | 1 | 3 | 2 | 2 | 3097.57 | 0.501 + 01 | 0.421 − 02 |
| *Q* branch | | | | | | | | |
| 4 | 1 | 3 | 4 | 2 | 2 | 3160.82 | 0.559 + 01 | 0.714 − 02 |
| 2 | 0 | 2 | 2 | 1 | 1 | 3184.64 | 0.987 + 01 | 0.472 − 02 |
| 2 | 1 | 1 | 2 | 0 | 2 | 3234.30 | 0.108 + 02 | 0.450 − 02 |
| *R* branch | | | | | | | | |
| 4 | 0 | 4 | 3 | 1 | 3 | 3275.47 | 0.850 + 01 | 0.489 − 02 |
| 3 | 1 | 3 | 2 | 0 | 2 | 3277.63 | 0.112 + 02 | 0.461 − 02 |
| 5 | 1 | 5 | 4 | 0 | 4 | 3302.84 | 0.986 + 01 | 0.782 − 02 |
| Vibrational transition 001–000 | | | | | | | | |
| *P* branch | | | | | | | | |
| 5 | 0 | 5 | 6 | 0 | 6 | 3140.36 | 0.249 + 02 | 0.556 − 01 |
| 4 | 1 | 4 | 5 | 1 | 5 | 3159.71 | 0.325 + 02 | 0.431 − 01 |
| 3 | 2 | 1 | 4 | 2 | 2 | 3160.75 | 0.211 + 02 | 0.269 − 01 |
| *Q* branch | | | | | | | | |
| 4 | 4 | 1 | 4 | 4 | 0 | 3236.52 | 0.178 + 02 | 0.595 − 01 |
| 4 | 3 | 2 | 4 | 3 | 1 | 3242.76 | 0.177 + 02 | 0.329 − 01 |
| 3 | 3 | 0 | 3 | 3 | 1 | 3244.29 | 0.354 + 02 | 0.438 − 01 |
| *R* branch | | | | | | | | |
| 2 | 1 | 2 | 1 | 1 | 1 | 3290.78 | 0.359 + 02 | 0.131 − 01 |
| 3 | 0 | 3 | 2 | 0 | 2 | 3313.27 | 0.563 + 02 | 0.230 − 01 |
| 4 | 1 | 4 | 3 | 1 | 3 | 3326.07 | 0.533 + 02 | 0.302 − 01 |
| Vibrational transition 030–000 | | | | | | | | |
| *P* branch | | | | | | | | |
| 5 | 1 | 5 | 6 | 2 | 4 | 3859.92 | 0.283 − 04 | 0.968 − 07 |
| 6 | 2 | 4 | 7 | 3 | 5 | 3938.36 | 0.255 − 04 | 0.214 − 06 |
| 3 | 1 | 3 | 4 | 2 | 2 | 3944.66 | 0.156 − 03 | 0.160 − 06 |

TABLE IX (*continued*).

| $J'$ | $K'_a$ | $K'_c$ | $J''$ | $K''_a$ | $K''_c$ | $\Delta E(\mathrm{cm}^{-1})$ | $S(\mathrm{atm}^{-1}\,\mathrm{cm}^{-2})$ | $R^2(\mathrm{a.u.}^2)$ |
|---|---|---|---|---|---|---|---|---|
| *Q* branch | | | | | | | | |
| 5 | 1 | 5 | 5 | 2 | 4 | 4013.11 | 0.509 – 03 | 0.804 – 06 |
| 3 | 1 | 3 | 3 | 2 | 2 | 4036.17 | 0.708 – 03 | 0.457 – 06 |
| 4 | 0 | 4 | 4 | 1 | 3 | 4038.34 | 0.981 – 03 | 0.789 – 06 |
| *R* branch | | | | | | | | |
| 4 | 0 | 4 | 3 | 1 | 3 | 4151.82 | 0.168 – 02 | 0.765 – 06 |
| 6 | 0 | 6 | 5 | 1 | 5 | 4193.37 | 0.183 – 02 | 0.183 – 05 |
| 5 | 1 | 5 | 4 | 0 | 4 | 4197.62 | 0.207 – 02 | 0.129 – 05 |

[a] See the text for definitions.

## VI. CONCLUSIONS

This contributions represents an attempt towards an accurate and compact characterization of the electronic ground state of the $H_2O^+$ ion by means of its near equilibrium potential energy and electric dipole moment functions. Our *ab initio* rotationally resolved spectra have enabled a detailed and direct comparison with the existing experimental spectral data. An advantage of such an approach is that any part of the rovibrational spectrum can be calculated. The obvious disadvantage, however, are the very small but—in terms of spectroscopic accuracy—still significant residual errors. The theoretical vibrational band origins agree with experiment to within a few wavenumbers for energies up to about 5000 $\mathrm{cm}^{-1}$ above the vibrational ground state, the theoretical rotational term values within the vibra-

TABLE X. Comparison of some theoretical and experimental rovibrational transition energies.

| $J'$ | $K'_a$ | $K'_c$ | $J''$ | $K''_a$ | $K''_c$ | This work $\Delta E(\mathrm{cm}^{-1})$ | Experimental $\Delta E(\mathrm{cm}^{-1})$ | $\Delta$ $(\mathrm{cm}^{-1})$ |
|---|---|---|---|---|---|---|---|---|
| Vibrational transition 000–000 | | | | | | | | |
| 2 | 1 | 1 | 1 | 1 | 1 | 49.71 | 49.538[a] | 0.17 |
| 3 | 2 | 2 | 2 | 2 | 0 | 62.02 | 62.034 | 0.01 |
| 4 | 3 | 2 | 3 | 3 | 0 | 84.67 | 84.593 | 0.08 |
| 4 | 3 | 1 | 3 | 3 | 1 | 85.09 | 85.172 | 0.08 |
| 4 | 2 | 2 | 3 | 2 | 2 | 91.50 | 91.321 | 0.18 |
| 5 | 1 | 5 | 3 | 1 | 3 | 166.36 | 166.703 | 0.34 |
| 6 | 0 | 6 | 4 | 0 | 4 | 205.44 | 205.972 | 0.53 |
| Vibrational transition 010–000 | | | | | | | | |
| 4 | 0 | 4 | 5 | 1 | 5 | 1312.26 | 1309.9389[b] | 2.32 |
| 1 | 1 | 1 | 2 | 2 | 0 | 1315.38 | 1313.3284 | 2.05 |
| 4 | 0 | 4 | 4 | 1 | 3 | 1365.15 | 1363.5670 | 1.58 |
| 0 | 0 | 0 | 1 | 1 | 1 | 1372.99 | 1371.2170 | 1.77 |
| 3 | 0 | 3 | 3 | 1 | 2 | 1377.03 | 1375.3245 | 1.90 |
| 1 | 1 | 1 | 0 | 0 | 0 | 1452.07 | 1450.8505 | 1.22 |
| 2 | 1 | 2 | 1 | 0 | 1 | 1468.57 | 1466.3464 | 2.22 |
| 4 | 2 | 2 | 4 | 1 | 3 | 1471.68 | 1469.9915 | 1.690 |
| 4 | 0 | 4 | 3 | 1 | 3 | 1478.62 | 1476.6780 | 1.94 |
| Vibrational transition 001–000 | | | | | | | | |
| 6 | 0 | 6 | 5 | 0 | 5 | 3140.36 | 3142.818[c] | 2.46 |
| 5 | 0 | 5 | 4 | 0 | 4 | 3158.01 | 3161.025 | 3.02 |
| 5 | 1 | 5 | 4 | 1 | 4 | 3159.71 | 3162.670 | 2.96 |
| 4 | 3 | 1 | 3 | 3 | 0 | 3159.13 | 3163.096 | 3.97 |
| 2 | 1 | 1 | 3 | 1 | 2 | 3321.44 | 3325.061 | 3.62 |
| 3 | 1 | 3 | 4 | 1 | 4 | 3326.07 | 3329.373 | 3.30 |
| 3 | 3 | 1 | 4 | 3 | 2 | 3327.92 | 3331.948 | 4.03 |
| 3 | 2 | 2 | 4 | 2 | 3 | 3331.04 | 3334.636 | 3.60 |
| 4 | 0 | 4 | 5 | 0 | 5 | 3345.80 | 3348.789 | 2.99 |
| 5 | 1 | 5 | 6 | 1 | 6 | 3359.91 | 3361.257 | 1.35 |

[a] Combination differences from Ref. 9.
[b] Reference 19.
[c] Reference 9.

TABLE XI. comparison of line intensity patterns.

| This Work | | | | | | | | Ref. 2 | |
|---|---|---|---|---|---|---|---|---|---|
| $J'$ | $K'_a$ | $K'_c$ | $J''$ | $K''_a$ | $K''_c$ | $\Delta E(\text{cm}^{-1})$ | $R^2$(debye) | $\Delta E(\text{cm}^{-1})$ | $S_i$[a] |
| Vibrational transition 000–000 | | | | | | | | | |
| 2 | 2 | 0 | 3 | 1 | 3 | 5.30 | 0.719 | 5.53 | 0.12 |
| 4 | 1 | 4 | 3 | 2 | 1 | 3.94 | 1.111 | 3.98 | 0.19 |
| 3 | 3 | 0 | 4 | 2 | 3 | 7.50 | 0.781 | 8.09 | 0.13 |
| 4 | 2 | 2 | 3 | 3 | 1 | 1.14 | 0.848 | 0.79 | 0.14 |
| 6 | 3 | 3 | 5 | 4 | 2 | 9.53 | 1.684 | 8.56 | 0.28 |
| 6 | 5 | 2 | 7 | 4 | 3 | 3.31 | 1.478 | 2.83 | 0.24 |
| Vibrational transition 010–000 | | | | | | | | | |
| 2 | 0 | 2 | 3 | 1 | 3 | 1340.74 | 0.107 | 1338.52 | 2.11 |
| 3 | 1 | 3 | 4 | 0 | 4 | 1345.34 | 0.114 | 1343.14 | 2.56 |
| 1 | 0 | 1 | 2 | 1 | 2 | 1356.02 | 0.079 | 1353.86 | 1.50 |
| 2 | 1 | 2 | 3 | 0 | 3 | 1367.39 | 0.068 | 1365.33 | 1.54 |
| 0 | 0 | 0 | 1 | 1 | 1 | 1372.99 | 0.054 | 1370.81 | 1.00 |
| 3 | 0 | 3 | 3 | 1 | 2 | 1377.03 | 0.158 | 1375.11 | 2.55 |
| 2 | 0 | 2 | 2 | 1 | 1 | 1385.04 | 0.127 | 1383.03 | 2.21 |
| 1 | 1 | 1 | 2 | 0 | 2 | 1390.09 | 0.029 | 1388.19 | 0.67 |
| 1 | 0 | 1 | 1 | 1 | 0 | 1389.80 | 0.082 | 1387.66 | 1.50 |
| 1 | 1 | 0 | 1 | 0 | 1 | 1435.37 | 0.065 | 1433.47 | 1.50 |
| 2 | 0 | 2 | 1 | 1 | 1 | 1434.76 | 0.034 | 1432.61 | 0.67 |
| 2 | 1 | 1 | 2 | 0 | 2 | 1440.02 | 0.093 | 1437.93 | 2.21 |
| 3 | 1 | 2 | 3 | 0 | 3 | 1448.07 | 0.104 | 1445.81 | 2.55 |
| 1 | 1 | 1 | 0 | 0 | 0 | 1452.07 | 0.044 | 1450.22 | 1.00 |
| 3 | 0 | 3 | 2 | 1 | 2 | 1457.04 | 0.076 | 1454.96 | 1.54 |
| 2 | 1 | 2 | 1 | 0 | 1 | 1468.57 | 0.067 | 1466.69 | 1.50 |
| 4 | 0 | 4 | 3 | 1 | 3 | 1478.62 | 0.125 | 1476.52 | 2.56 |
| 3 | 1 | 3 | 2 | 0 | 2 | 1483.20 | 0.096 | 1481.28 | 2.11 |

[a] Relative line intensity pattern.

tional states exhibit errors in the range from 0.01 to about 1 $\text{cm}^{-1}$. The theoretical absolute line intensities are expected to be accurate to within 10%–20%. It is hoped that more complete experimental information combined with the present results will lead to further improvements of the electronic ground state potential energy and electric dipole moment functions of the $H_2O^+$ ion.

## ACKNOWLEDGMENTS

This work has been supported by the Deutsche Forschungsgemeinschaft and Fonds der Chemischen Industrie, SERC and Electronic Data System, Rüsselsheim. The fits and perturbational calculations have been performed with the SURFIT program of J. Senekowitsch. His help during the course of this work is gratefully acknowledged. We are thankful to R. Stickland, P. Brown, and P. Davies for providing us with their unpublished data and for stimulating discussions.

[1] H. Lew and I. Heiber, J. Chem. Phys. **58**, 1246 (1973).
[2] H. Lew, Canad. J. Phys. **54**, 2028 (1976).
[3] H. Lew and R. Groleau, Can. J. Phys. **65**, 739 (1987).
[4] S. Leutwyler, D. Klapstein, and J. P. Maier, Chem. Phys. **74**, 441 (1983).
[5] M. Tsuji, J. P. Maier, H. Obase, and Y. Nishiruma, Chem. Phys. Lett. **147**, 619 (1988).
[6] A. Carrington, D. R. J. Milverton, P. G. Roberts, and P. J. Sarre, J. Chem. Phys. **68**, 5639 (1978).
[7] S. E. Strahan, R. P. Mueller, and R. J. Saykally, J. Chem. Phys. **85**, 1252 (1986).
[8] D. J. Liu, W. Ch. Ho, and T. Oka, J. Chem. Phys. **87**, 2442 (1987).
[9] B. M. Dinelli, M. W. Crofton, and T. Oka, J. Mol. Spectrosc. **127**, 1 (1988).
[10] J. E. Reutt, L. S. Wang, Y. T. Lee, and D. A. Shirley, J. Chem. Phys. **85**, 6928 (1986).
[11] R. N. Dixon, G. Duxbury, J. W. Rabalais, and L. Asbrink, Mol. Phys. **31**, 423 (1976).
[12] L. Karlsson, L. Mattson, R. Jadrny, R. G. Albridge, S. Pinchas, T. Bergmark, and K. Siegbahn, J. Chem. Phys. **62**, 4745 (1975).
[13] B. Friedrich, G. Niedner, M. Noll, and J. P. Toennies, J. Chem. Phys. **87**, 5256 (1987).
[14] B. Friedrich, G. Niedner, M. Noll, and J. P. Toennies, J. Chem. Phys. **87**, 1447 (1987).
[15] K. T. Gillen, B. H. Mahan, and J. S. Winn, J. Chem. Phys. **59**, 6380 (1973).
[16] H. H. Harris and J. J. Leventhal, J. Chem. Phys. **64**, 3185 (1976).
[17] A. J. Lorquet and J. C. Lorquet, Chem. Phys. **4**, 353 (1974).
[18] K. H. Tan, C. E. Brion, Ph.E. van der Leeuw, and M. J. van der Wiel, Chem. Phys. **29**, 299 (1978).
[19] R. Strickland, P. Brown, and P. Davies (to be published).
[20] Ch. Jungen, K.-E. J. Hallin, and A. J. Merer, Mol. Phys. **40**, 25 (1980).
[21] A. Degli Esposti, D. G. Lister, P. Palmieri, and C. Degli Esposti, J. Chem. Phys. **87**, 6772 (1987).
[22] Ch. J. Jackels, J. Chem. Phys. **72**, 4873 (1980).
[23] J. A. Smith, P. Jorgensen, and Y. Ohrn, J. Chem. Phys. **62**, 1285 (1975).

[24]P. J. Fortune, B. J. Rosenberg, and A. C. Wahl, J. Chem. Phys. **65**, 2201 (1976).
[25]S. Carter and N. C. Handy, Mol. Phys. **57**, 175 (1986).
[26]S. Carter, J. Senekowitsch, N. C. Handy, and P. Rosmus, Mol. Phys. **65**, 143 (1988).
[27]P. Rosmus, B. Weis, S. Carter, H.-J. Werner, and P. J. Knowles (to be published).
[28]S. Carter and N. C. Handy, Mol. Phys. **52**, 1367 (1984).
[29]F. B. van Duijneveldt, IBM Research Report No. RJ945, 1971.
[30]H.-J. Werner and P. J. Knowles, J. Chem. Phys. **89**, 5803 (1988).
[31]P. J. Knowles and H.-J. Werner, Chem. Phys. Lett. **145**, 514 (1988).
[32]H.-J. Werner and P. J. Knowles, J. Chem. Phys. **82**, 5053 (1985).
[33]P. J. Knowles and H.-J. Werner, Chem. Phys. Lett. **115**, 259 (1985).
[34]H. H. Nielsen in *Flügge, Handbuch der Physik* (Springer, Berlin, 1959), Vol. 37.
[35]I. M. Mills, in *Molecular Spectroscopy; Modern Research*, edited by K. N. Rao and C. W. Matthews (Academic, New York, 1972).
[36]I. M. Mills, *Specialist Reports Theoretical Chemistry* (The Chemical Society, London, 1974), Vol. 1.
[37]W. Gordy and R. L. Cook, *Microwave Molecular Spectra* (Wiley, New York, 1984).
[38]C. Camy-Peyret and J.-M. Flaud, in *Molecular Spectroscopy: Modern Research*, edited by K. N. Rao (Academic, New York, 1985), Vol. III.
[39]S. Carter, N. C. Handy, and B. T. Sutcliffe, Mol. Phys. **49**, 745 (1983).
[40]S. Carter and N. C. Handy, J. Chem. Phys. **87**, 4294 (1987).
[41]T. R. Dyke and J. S. Muenter, J. Chem. Phys. **59**, 3125 (1973).
[42]M. Henniger, S. Fenistein, M. Durup-Ferguson, E. E. Ferguson, R. Marx, and G. Mauclaire, Chem. Phys. Lett. **131**, 439 (1986).
[43]J. W. C. Johns, J. Mol. Spectrosc. **125**, 442 (1987).
[44]L. L. Strow, J. Quant. Spectrosc. Radiat. Transfer **29**, 395 (1983).